Enclosure Design for an Automated Vacuum Application

Mario R. Flores Milán
Master of Engineering in Mechanical Engineering
Advisor: Julio Noriega Motta, Ph.D.
Mechanical Engineering Department
Polytechnic University of Puerto Rico

Abstract *—The plastic injection industries make use of the Deflashing Machine, which requires to recycle the filter that collects the plastic shaving dust, down to 0.2um. A series of automated subsystems, located in portable frame table, were already designed with the purpose to remove dust from the filter using jet air nozzles and collecting it with a dust collector. The only system not yet designed was an enclosed system with capacity to isolate the plastic dust from the atmosphere and to hold a given external pressure load, caused from vacuum pressure, of 15 Psi. A design concept was made, then optimized with the use of plates theory, comparing stress and deflection results with computer aided engineering and design (CAE/D). The results of the finished design provided an enclosed system with 1.5 safety factor, 88% deflection decrease from the conceptual design and which consumed only 19.4% of the general budget ($21,000).*

Key Terms *— Finite Element Analysis, Large Deflection, Plate Theory, Vacuum Pressure.*

PROBLEM STATEMENT

The plastic injection molding industry makes use of the Deflashing Machine, which has a primary function of removing the fine dust and plastic shavings of plastic mold parts. The machine collects the dust by using a cylindrical filter, that has the potential to be recycled to minimize operational cost. The main goal is to facilitate a more cost-effective and unharmful way to recycle the filter by cleaning it without exposing the workforce and the atmosphere to harmful dust particles. A mechanical design, comprised of custom sheet metal enclosure, will be needed to allocate the cylindrical filter. The enclosure will be placed in a predetermined station, that has connection ports to work alongside other subsystems. In this case, a provided stationary jet air manifold and dust collector manifold system to remove and collect the dust from the filter, respectively. The problem arises when the suction manifold is subjecting the enclosure to an external pressure of 15 Psi. The cabin will not only trap the particle dust but will also be able to withstand the external pressure to avoid deformation. The enclosure alongside the other existing subsystems will provide a practical approach that results in a cost-efficient and eco-friendly solution.

Research Objectives

- Develop a manufacturable system, able to maintain below the budget of $4,750 and a factor of safety (FOS) around 1.5.
- Design an enclosed system to protect the workforce and atmosphere from 0.2μm fine dust particles.
- Design a structural reliable enclosure, able to withstand 15 Psi. of external static pressure.

Research Contributions

The primary objective of the project is to provide an economic structurally sound enclosure system for the cleaning system that protects the workers and the atmosphere from plastic waste. In addition, provide a safe and simple to manufacture equipment that would assist the user during his working process. The result of this project will help increase the awareness of the leaders of the plastic industries to rise the standards and the quality of the cleaning process.

RESEARCH BACKGROUND

The Deflashing Machine, advise the operator to remove the cylindrical filter, as shown in Figure 1.

Once the operator removes the cylindrical filter, the operator will go to an "isolated" location to dust off the plastic waste with a jet air gun. All this procedure creates undesirable health hazards and spreads unwanted plastic dust waste to the air.

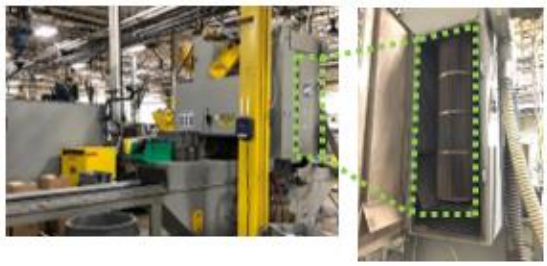

Figure 1
Deflashing Machine and Filter

In order to start developing the concept, the dimensions of the filter (Figure 2) are critical to establish the space constraint of the cabin.

Figure 2
Filter Dimensions (All Dimensions are in Inches)

Conceptual Design

To design for manufacture, the enclosure will make use of available and cost-effective metals like steel or stainless steel. The manufacture procedure will involve conventional sheet metal work like welding, water jet cutting and metal bending.

The dimensions of 18.00", 56.278" and 22.19", as shown in Figure 3, are the initial information of the space constraints that is desirable to allocate the enclosure to a determined portable frame structure.

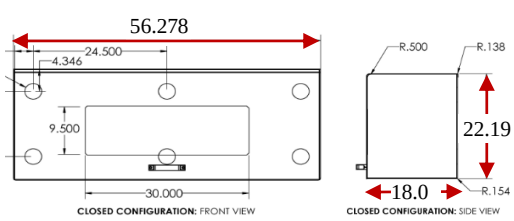

Figure 3
Enclosure System Design Concept Schematics

Selecting this type of geometry will cause mechanical stresses in the abrupt changes, such as the edges due to vacuum pressure. In conjunction with the stress, there will be unwanted deflection in the center of the plates.

The combination of computer aided design, finite element analysis and mechanics of materials is critical to design a functional enclosed system. Questions such as the following will need to be answered:

1. What are the maximum stresses (in Psi.) for each face of the enclosure?
2. Which stress (in Psi.) is critical where is it located?
3. What will be the maximum deflection (in inches) for each face of the enclosure?

Flat Plates

An advantageous starting strategy is to model the enclosure system as a simple and closed rectangular box. This simplifies the analysis to focus on each face as a rectangular flat plate with fixed edges. Calculating the stresses and deflection for each face, informs beforehand the affected adjacent components.

From a definition standpoint, a plate (see Figure 4) is a body with two plane surfaces (faces) separated in small distance with prismatic lateral surfaces [1].

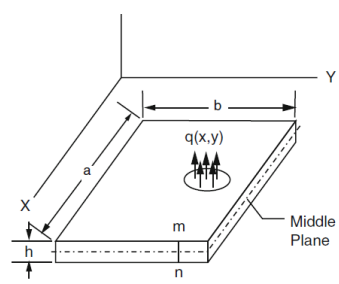

Figure 4
Representation of a Thin Plate [2]

That small distance is called the thickness (h), which is significantly smaller than the width (b) and length (a). The projection of the midpoints that form a plane in the middle of the thickness, is known as the midplane. The edges are known as the closed line bounding the midplane of the plate [1]. For loaded transverse surfaces, the classification of plates is

imperative to develop the correct assumptions and analysis [2]. The plate is thin if the thickness of the plate is very small, $h/b < 0.001$. For thin plates, membrane forces along with twisting and bending moments are crucial to deliver equilibrium mobilizing finite deformations. Three dimensional effects are important for the case of a thick plate $h/b > 0.4$ [2].

Other descriptions of the plates are critical, for instance, the distance between the two faces remain constant (constant thickness) or do not remain constant (variable thickness) [3]. Many theories have been developed to determine small or large lateral deflection ($\boldsymbol{w}$) of the plate in z direction. When $\boldsymbol{w} < \mathbf{h/2}$, small-deflection theory is applied, if $\boldsymbol{w} > \mathbf{h/2}$, then large displacements theory must be applied [3].

Large Deflection of Plates (All Edges Fixed)

There are different theories that approximate the stresses and strains values for each unique condition of a plate. It is proposed, that for the given dimensions in the conceptual design (see Figure 3) and loading conditions (15 Psi of external pressure), each face of the enclosure system will be classified as thin plate with large deflection theory with fixed edges. This theory application will yield values of stress, the maximum stress and the maximum deflection for each face, where it will be supported with finite element analysis.

A single-linear equation describes small deflection of a flat plate [4]. Large deflection is described as nonlinear terms for equilibrium conditions and are described by two fourth-order, second-degree, partial differential equations [4]. Large displacements involve stretching at the center of the surface and consequent tensions, where is interacting with the curvatures [4]. To begin with, the large deflection-theory of flat plates with uniform thickness is governed by Föppl–Von Kármán equations (1-2) and the general equations and strain developed by Timoshenko [5],

$$\frac{\partial^4 F}{\partial x^4} + 2\frac{\partial^4 F}{\partial x^2\,\partial y^2} + \frac{\partial^4 F}{\partial y^4} = E\left[\left(\frac{\partial^2 w}{\partial x\,\partial y}\right)^2 - \frac{\partial^2 w}{\partial x^2}\frac{\partial^2 w}{\partial y^2}\right] \quad (1)$$

$$\frac{\partial^4 w}{\partial x^4} + 2\frac{\partial^4 w}{\partial x^2\,\partial y^2} + \frac{\partial^4 w}{\partial y^4} = \frac{q}{D} + \frac{h}{D}\left(\frac{\partial^2 F}{\partial y^2}\frac{\partial^2 w}{\partial x^2} + \frac{\partial^2 F}{\partial x^2}\frac{\partial^2 w}{\partial y^2} - 2\frac{\partial^2 F}{\partial x\,\partial y}\frac{\partial^2 w}{\partial x\,\partial y}\right) \quad (2)$$

where the median-fiber stresses (3) and strains (4) are:

$$\sigma'_x = \frac{\partial^2 F}{\partial x^2}, \quad \sigma'_y = \frac{\partial^4 F}{\partial y^4}, \quad \tau'_{x,y} = -\frac{\partial^4 F}{\partial x\,\partial y} \quad (3)$$

$$\varepsilon'_x = \frac{1}{E}\left(\frac{\partial^2 F}{\partial y^2} - \mu\frac{\partial^2 F}{\partial x^2}\right), \ \varepsilon'_y = \frac{1}{E}\left(\frac{\partial^2 F}{\partial x^2} - \mu\frac{\partial^2 F}{\partial y^2}\right), \ \gamma'_{x,y} = -\frac{2(1+\mu)}{E}\frac{\partial^2 F}{\partial x\,\partial y} \quad (4)$$

F – Stress function
w – Normal displacement at the middle surface
$\sigma'_x, \sigma'_y, \tau'_{x,y}$ – Membrane stresses in middle surface
$\varepsilon'_x, \varepsilon'_y, \tau'_{x,y}$ – Membrane strain in middle surface
E – Modulus of elasticity (material constant)
μ – Poisson's ratio (material constant)
q – Normal pressure
D – Flexural rigidity of plate:

$$D = \frac{Eh^3}{12\,(1-\mu^2)} \quad (5)$$

From the studies, there are three way of analyzing plates with large deflections [4]. Only one from the three cases will be evaluated, with key assumption that all faces of the enclosure is subjected to lateral loading perpendicular to the plane of the plates, but no side thrust is applied in the plane of the plates [4]. For a plate with built-in edges or clamped, the boundary conditions are expressed by the equation (6), if the x-axis coincides with the clamp edge and equation (7) if the y-axis coincide with the clamped edge. If the edge is rigidly clamped, preventing any displacement along its supports, then the strain is zero along that edge at the median fibers, as shown in the equations (6-9) [4],

$$(w)_{y=0} = 0, \ \left(\frac{\partial w}{\partial y}\right)_{y=0} = 0 \quad (6)$$

$$(w)_{x=0} = 0, \ \left(\frac{\partial w}{\partial x}\right)_{x=0} = 0 \quad (7)$$

$$(\varepsilon_y{}')_{x=0} = 0 \quad (8)$$

$$(\varepsilon_x{}')_{y=0} = 0 \quad (9)$$

Solution methods have been developed from Von Karman equations, specifically for the case of a fixed rectangular thin plate subjected to uniform distributed pressure and is given by Chi-Teh Wang [4]. These methods provide approximate solutions for a Poisson's ratio $\boldsymbol{\mu}$ = 0.3, where dimensionless coefficient tables and direct solution equations will be useful during the design methodology chapter [6].

DESIGN METHODOLOGY

The conceptual design, as illustrated in Figure 3 provides vital geometry conditions, while simultaneously providing the design working pressure of the enclosure system. During the procedure, unknown variables were presented, which will become the standard design criterion. The unknown variables are as follows:

- Maximum deflection (in) – $\boldsymbol{w_{max}}$
- Stress at the center (Psi.) – $\boldsymbol{\sigma_0}$
- Maximum stress (Psi.) – $\boldsymbol{\sigma_{max}}$

Once the maximum stress (at the long edges), maximum deflection and stress at the center for each face of the enclosure is known, a possible design optimization will be applied. The assumptions and conditions will follow the fundamental concepts of large deflection theory for fixed rectangular plate. Equations (1-9) will not be used directly, however they represent the foundation for the proceeding equations in this chapter. It is expected to see maximum stresses at the center of the plate's long edge and maximum deflection at the center of the plate.

Information Breakdown

From a solution strategy standpoint, displaying a breakdown of the given information will work as the baseline for the development of assumptions and conditions. Figure 5 represents a simple model of the enclosure system and shows the uniform distributed load caused from the external pressure due to the inside vacuum.

1. Shape of the Vacuum Chamber – Rectangular Box
2. Design Pressure (**q**) = 15 Psi. (Uniform Distributed Load)
3. Sheet Metal Thickness (**h**) = 7/64 inches (Gauge 12)
4. Material – Stainless Steel 304 (**E** = 29000 Ksi., **μ** = 0.3)
5. Length (**I**) = 56.278 in
6. Width (**B**) = 18.00 in
7. Height (**H**) = 22.19 in

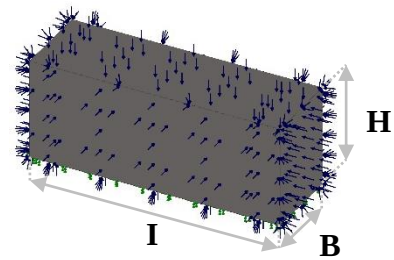

Figure 5
Enclosure Study Model

Assumptions and Conditions

As shown in Figure 6, an explosion view was created from a rectangular box study model. The exploded view helps demonstrate the conditions for each face of the enclosure. The green arrows represent that all edges for each face are fixed. The uniform transverse distributed load (q), is defined for each face by blue arrows.

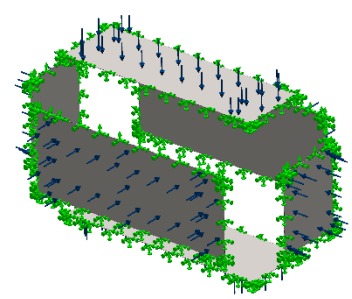

Figure 6
Explosion View of the Enclosure Study Model

Before proceeding to the application of the defined equations, a clear understanding with the assumptions and conditions is essential to yield accurate calculations. The analysis is going to be developed under the following assumptions and conditions:

1. The working design pressure will not entirely collapse the system, but it will deflect each face of the enclosure with the same magnitude of pressure.
2. Isotropic and homogeneous material.
3. The edges of the plates are fixed, where deflection is zero [4]. The plane that is tangent to the deflected middle surface along this edge coincides with the initial position of the middle plane of the plate and follows the boundary equations (6-9) [4].
4. Only lateral loading perpendicular to the plate will be applied, but no side thrust will be present in the plane of the plates [4].
5. "Lines normal to the middle surface before deformation remains to the middle surface after deformation" [4].
6. Deflections are large with respect of the thickness of the plate but are still small with respect to the other dimensions [4].
7. "The normal stress perpendicular to the faces of the plate is negligible in comparison with the other normal stresses" [4].
8. The stress and displacement of the side faces of the enclosure will be equal, the same applies for the front-back and top-bottom faces.

Solution Strategy

Roark's equations (see [6]) were developed by solving the Föppl–Von Kármán equations (1-2), specifically for the previously mentioned assumptions and conditions. The relations among load (**q**), deflection ($\boldsymbol{w}_{\mathbf{max}}$), and stresses ($\boldsymbol{\sigma}_{\mathbf{max}}$ and $\boldsymbol{\sigma}_{\mathbf{o}}$) are expressed for a Poisson's ratio of $\boldsymbol{\mu}$ = 0.3 by numerical values of dimensionless coefficients (10-13) [6].

$$\text{Pressure Ratio} \rightarrow K_1 = \frac{qb^4}{Eh^4} \qquad (10)$$

$$\text{Center Deflection Ratio} \rightarrow K_2 = \frac{w_{max}}{h} \qquad (11)$$

$$\text{Stress Ratio at Center} \rightarrow K_3 = \frac{\sigma_o b^2}{Eh^2} \qquad (12)$$

$$\text{Maximum Stress Ratio} \rightarrow K_4 = \frac{\sigma_{max} b^2}{Eh^2} \qquad (13)$$

Figure 7 identifies the theoretical location of stresses, deflection and the corresponding dimension designation. The green dotted line indicates where the maximum stress ($\boldsymbol{\sigma}_{\mathbf{max}}$) is located, which is at the center of the long edges. The red dotted line indicates the maximum deflection at the center and the stress at the center ($\boldsymbol{\sigma}_{\mathbf{o}}$). Each face of the study model (Figure 4) of the enclosure system is going to be analyzed with the previous set of equations (10-13) and fixed edge conditions. The results will determine if future optimization of the conceptual design (Figure 3) is required.

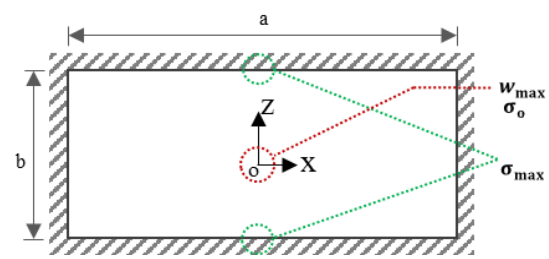

Figure 7
Uniform Loaded Rectangular Fixed Plate [6]

The values of span-width ratio will define, for each plate, the numerical values from the Roark's table. Therefore, the ratio of the larger span length (**a**) with respect to the short span length (**b**) for each plate is given by [6]:

$$\text{Top and Bottom} \rightarrow \frac{a}{b} = \frac{56.278\text{ in}}{18.000\text{ in}} = 3.127 \qquad (14)$$

$$\text{Side Plates} \rightarrow \frac{a}{b} = \frac{22.190\text{ in}}{18.000\text{ in}} = 1.233 \qquad (15)$$

$$\text{Front and Back} \rightarrow \frac{a}{b} = \frac{56.278\text{ in}}{22.190\text{ in}} = 2.53 \qquad (16)$$

If the ratio between the larger span and the shorter span (**a/b**) ≥ 2 then, (**a/b**) = ∞ [6]. With this condition and for a determined pressure ratio ($\mathbf{K_1}$), the non-dimensional values of $\mathbf{K_2}$, $\mathbf{K_3}$ and $\mathbf{K_4}$ can be directly obtain from the Roark's table [6]. This table is specifically designed for the case of large deflected rectangular plates, where it has a limited range of pressure ratios values. The coefficient values of the proceeding Table 1 is an extraction of the Roark's table [6]. These coefficients values only work for the case of a fixed configuration and for

span-width ratio of 1.5 to ∞, where for analytical purposes the side plates will be analyzed within this range.

Table 1
Deflection and Stresses Coefficients [6]

Rectangular Fixed Plates Under Uniform Load				
a/b		**1.5 to ∞**		
Coefficients		$\frac{w}{h}$	$\frac{\sigma_o b^2}{Eh^2}$	$\frac{\sigma_{max} b^2}{Eh^2}$
$\frac{qb^4}{Eh^4}$	**0**	0.0000	0.0000	0.0000
	12.5	0.2800	0.2000	5.7500
	25	0.5100	0.6600	11.1200
	50	0.8250	1.9000	20.3000
	75	1.0700	3.2000	27.8000
	100	1.2400	4.3500	35.0000
	125	1.4000	5.4000	41.0000
	150	1.5000	6.5000	47.0000
	175	1.6300	7.5000	52.5000
	200	1.7200	8.5000	57.6000
	250	1.8600	10.3000	67.0000

After the plate's dimensions are defined, the value for pressure ratio ($\mathbf{K_1}$) needs to be calculated for each plate before proceeding with any further calculation. These preliminary calculations will help determine if the pressure ratio coefficient for each plate is within the range of the given pressure ratios.

$$\text{Top and Bottom, } K_{1TB} = \frac{qb^4}{Eh^4} = \frac{15\ \text{Psi} * (18.000\ \text{in})^4}{29 * 10^6\ \text{Psi} * (0.1094\ \text{in})^4} = 379.065 \quad (17)$$

$$\text{Side Plates, } K_{1SP} = \frac{qb^4}{Eh^4} = \frac{15\ \text{Psi} * (18.000\ \text{in})^4}{29 * 10^6\ \text{Psi} * (0.1094\ \text{in})^4} = 379.065 \quad (18)$$

$$\text{Front and Back, } K_{1FB} = \frac{qb^4}{Eh^4} = \frac{15\ \text{Psi} * (22.19\ \text{in})^4}{29 * 10^6\ \text{Psi} * (0.1094\ \text{in})^4} = 875.494 \quad (19)$$

Neither of the previous results fall within the range of the provided pressure ratios of Table 1, this will mean that a form of extrapolation is required. The approximated values for when $\mathbf{K_1} > \mathbf{250}$ can be obtained by using a curve fitting tool for the given data. It is important to recall that safety is the primary concern, therefore the safety factor is increased due to the extrapolated values being slightly larger. The results will benefit the structural integrity of the enclosure and is obtain by substituting the pressure ratio in the x-variable of each curve fitting equation. The following plates integrates the nominal dimensions of the plates, free body diagrams and the nondimensional coefficients.

- Top and Bottom Plates

For $K_1 = \frac{qb^4}{Eh^4} = 379.0654$ and $a/b = 3.127$

$K_2 = \frac{w_{max}}{h} = 0.0658*(379.065)^{0.625} = 2.691$

$K_3 = \frac{\sigma_o b^2}{Eh^2} = 0.0434 * (379.065) - 0.1933 = 16.258$

$K_4 = \frac{\sigma_{max} b^2}{Eh^2} = 0.7926 * (379.065)^{0.8143} = 99.733$

- Side Plates

For $K_1 = \frac{qb^4}{Eh^4} = 379.065$ and $a/b = 1.233$

$K_2 = \frac{w_{max}}{h} = 0.0658*(379.065)^{0.625} = 2.691$

$K_3 = \frac{\sigma_o b^2}{Eh^2} = 0.0434 * (379.065) - 0.1933 = 16.258$

$K_4 = \frac{\sigma_{max} b^2}{Eh^2} = 0.7926 * (379.065)^{0.8143} = 99.733$

- Front and Back Plates

For $K_1 = \frac{qb^4}{Eh^4} = 875.494$ and $a/b = 2.53$

$K_2 = \frac{w_{max}}{h} = 0.0658*(875.494)^{0.625} = 4.541$

$K_3 = \frac{\sigma_o b^2}{Eh^2} = 0.0434 * (875.494) - 0.1933 = 37.803$

$K_4 = \frac{\sigma_{max} b^2}{Eh^2} = 0.7926 * (875.494)^{0.8143} = 194.358$

RESULTS AND OPTIMIZATION

The stresses and deflection for each plate are solved and compared with the finite element analysis tool from Solid Works. The results that are obtained from each plate is also compared to the uninsulated plate study model. From the results, an optimization

for the conceptual design of the enclsosure system is made by establishing a factor of safety (FOS) of 1.5, by considering manufacturability and cost-effectiveness.

Plate Results Study

The stresses and maximum deflection from each plate coefficients ($\mathbf{K_2, K_3, K_4}$) are solved as following:

- Top and Bottom Plates

$$w_{\max} = \mathrm{K_2 h} = 2.691 * 0.1094 \text{ in } = 0.295 \text{ in}$$

$$\sigma_o = \mathrm{K_3}\frac{\mathrm{Eh^2}}{\mathrm{b^2}} = 16.258 * \frac{29 * 10^6 \text{ Psi} * (0.1094 \text{ in})^2}{(18.000 \text{ in})^2} = 1.742 \times 10^4 \text{ Psi.}$$

$$\sigma_{\max} = \mathrm{K_4}\frac{\mathrm{Eh^2}}{\mathrm{b^2}} = 99.733 * \frac{29 * 10^6 \text{ Psi} * (0.1094 \text{ in})^2}{(18.000 \text{ in})^2} = 1.068 \times 10^5 \text{ Psi.}$$

- Side Plates

$$w_{\max} = \mathrm{K_2 h} = 2.691 * 0.1094 \text{ in } = 0.295 \text{ in}$$

$$\sigma_o = \mathrm{K_3}\frac{\mathrm{Eh^2}}{\mathrm{b^2}} = 16.258 * \frac{29 * 10^6 \text{ Psi} * (0.1094 \text{ in})^2}{(18.000 \text{ in})^2} = 1.742 \times 10^4 \text{ Psi.}$$

$$\sigma_{\max} = \mathrm{K_4}\frac{\mathrm{Eh^2}}{\mathrm{b^2}} = 99.733 * \frac{29 * 10^6 \text{ Psi} * (0.1094 \text{ in})^2}{(18.000 \text{ in})^2} = 1.068 \times 10^5 \text{ Psi.}$$

- Front and Back

$$w_{\max} = \mathrm{K_2 h} = 4.541 * 0.1094 \text{ in} = 0.497 \text{ in}$$

$$\sigma_o = \mathrm{K_3}\frac{\mathrm{Eh^2}}{\mathrm{b^2}} = 37.803 * \frac{29 * 10^6 \text{ Psi} * (0.1094 \text{ in})^2}{(22.19 \text{ in})^2} = 2.665 \times 10^4 \text{ Psi.}$$

$$\sigma_{\max} = \mathrm{K_4}\frac{\mathrm{Eh^2}}{\mathrm{b^2}} = 194.358 * \frac{29 * 10^6 \text{ Psi} * (0.1094 \text{ in})^2}{(22.19 \text{ in})^2} = 1.370 \times 10^5 \text{ Psi.}$$

Finite Element Analysis

Between the analytical method and finite methods tool, as shown in Figure 8 and Table 2, the stresses at the center, the maximum stresses and maximum deflection display a noticeable difference in the results. As expected, these differences are given by the extrapolation in the analytical method. Both methods show almost identical stresses and displacement results, however these stresses and deflection are unwanted for design purposes. Particularly, the maximum stress exceeds the yield strength of the material at the long edges for all the plates.

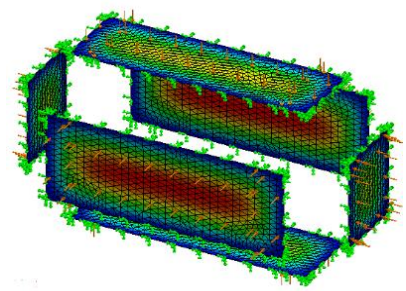

Figure 8
FEA Results for Insulated Plates Model

Table 2
Analytical Results and FEA Results

Analysis Method	Analytical Insulated Plates	FEA Insulated Plates
Stress at Center - σ_o (Psi)		
Top and Bottom	1.742E+04	2.525E+04
Sides	1.742E+04	2.296E+04
Front and Back	2.665E+04	3.635E+04
Maximum Stress - σ_{max} (Psi)		
Top and Bottom	1.07E+05	6.018E+04
Sides	1.07E+05	5.510E+04
Front and Back	1.37E+05	6.526E+04
Maximum Deflection - w_{max} (in)		
Top and Bottom	0.295	0.254
Sides	0.295	0.233
Front and Back	0.497	0.348

Uninsulated Plate Results Study

The analysis objective of the proceeding uninsulated plate model, as shown in Figure 9, is to provide some insight of the structural integrity of the system with nearly straight bends. With allowable bends of 0.0625" at the corners for a good mesh of the enclosure, it is expected that the model will

present approximate similar results to the study of insulated plate models.

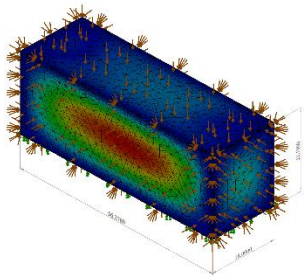

Figure 9
FEA Results for Uninsulated Plate Model

Both studies present a range of stresses that exceed the yield strength of the material (**Y** = 29.99 Ksi.). For example, for both studies, the maximum stress at the edges of the system falls between 6.526E+04 Psi. to 1.466E+05 Psi. Interestingly, it shows comparable results on the maximum deflection for each face of the enclosure, especially for the front and back plates. For instance, the maximum deflection of the uninsulated plate study model is 0.472" and is located at the front and back faces, where the insulated front and back plates model (Figure 7) is 0.497". The uninsulated model alone does not satisfy the objectives, a better reinforcement is required. For design purposes, the results from Table 2 and Table 3 provides what is needed to start the process of optimization on the structure.

Table 3
FEA Uninsulated Plates Results

FEA Uninsulated Plates			
Values	w_{max} **(in)**	σ_{max}**(Psi)**	σ_o **(Psi)**
Top and Bottom	0.118	7.338E+04	1.843E+04
Sides	0.157	5.506E+04	1.843E+04
Front and Back	0.472	1.466E+05	3.675E+04

Design Optimization

The conceptual enclosure is beyond the elastic limit of the stainless steel 304. "As the material is deformed beyond this point, the stress is no longer proportional to strain and permanent, nonrecoverable, or plastic deformation occurs [7]." "A structure or component that has plastically deformed or experienced a permanent change in shape may not be capable of functioning as intended [7]."

A budget of $4,750 was defined for the construction of the enclosure system, that constitutes 22.6% of the whole cleaning system budget. The initial enclosure concept was quoted $1,784.00 after taxes, this mean that there is room for upgrades that will provide a reliable and functional design. As previously stated in the results discussion, reinforcement will be needed to apply at the center and at the edges to eliminate large deflections and stresses on every side of the system. The proceeding optimization will consider viable cost-effective design techniques for available manufacture procedures, by maintaining a minimum factor of safety of 1.5. Also, it will take into account that the top plate and the frontal plate needs to be joined perpendicularly, to work as the access door to allow to take the filter in and out of the enclosure.

From various iterations with the application of computer aided design (CAD) and finite element analysis (FEA) software, a new enclosure was made. This was possible by reinforcing it with angular extrusion (2.125" x 2.125", 3/8" thick) framing. In addition, the angular frame material is S.S.304 and it provides manufacturing versatility and it will invade less the inside space constraints of the enclosure. The corresponding plates were assembled into the frame to test the structural integrity on each side, as shown in Figure 10.

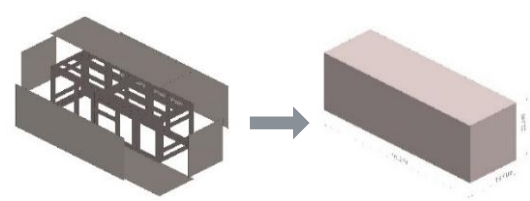

Figure 10
Framing Application

Once the model is defined, a finite element analysis is made, as shown in Figure 11, where it shows the stress distribution. The stresses presented in Figure 11 are below the material yield strength (2.999E+04 Psi.), with a maximum stress of

1.942E+04 Psi. This time, the maximum deflection in the system is 0.058”, almost half of the proposed of the material gauge.

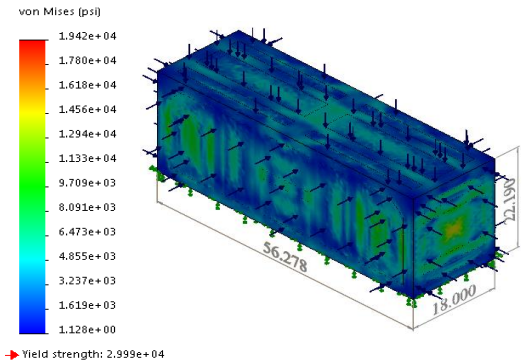

Figure 11
FEA Results for the Reinforced Enclosure

To obtain the exact minimum factor of safety, the yield strength of 2.999E+04 Psi. will be divided by the maximum stress value of 1.942E+04 Psi. which is used as the allowable stress in the proceeding calculation.

$$\mathrm{FOS} = \frac{\mathrm{Y}}{\sigma_{\mathrm{allow}}} = \frac{2.999\mathrm{E}+04}{1.942\mathrm{E}+04} = 1.54 \quad (20)$$

The FOS result satisfy the most important design objective, and the system is slightly modified for manufacturing purposes, as shown in Figure 12. Sheet metal design techniques along with the structural angular extrusion framing was essential to ensure structure integrity.

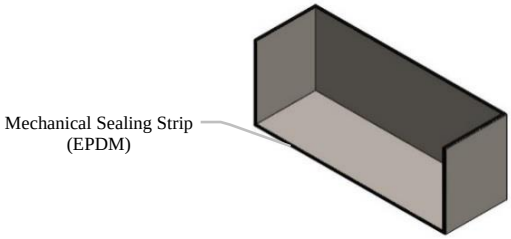

Figure 12
Application of Mechanical Sealing Strip

For manufacturability, the system was divided into five main parts as illustrated in Figure 13. The manufacture cost is $4,080. Besides a FOS of 1.5, the new design satisfies another project objective by maintaining below the budget, which is now 19% of the budget value ($21,000) of the whole automated machine.

A 1/16” recommended space was also added between the access door and the main base for an EPDM mechanical sealing strip. To ensure a proper mechanical sealing, a series of adjustable grip draw latch mechanism is built in, where it provides a 660 Lbs. holding capacity for each latch. The addition of these latching mechanism for the access door, provides more compatibility to the fixed edges plates studies. Figure 13 shows the setting of the mechanical strip and Figure 14 illustrate the locations of the draw latch mechanism.

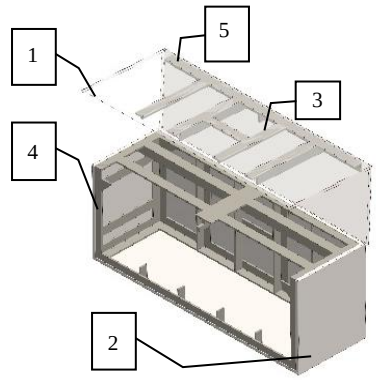

Figure 13
Parts of the New Enclosure System

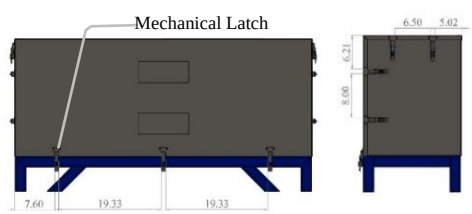

Figure 14
Application of Mechanical Latches

CONCLUSIONS AND RECOMMENDATIONS

The reinforced enclosure system satisfied all the proposed objectives and was successfully integrated with the other defined subsystems, as shown in Figure 15. This was achieved by modeling the enclosure to a rectangular box and studying each face as a fixed edges plate. For the given load and material properties, assumptions and conditions were made to apply the theory of large deflection for fixed plates. This approach was crucial to understand and predict where the critical stresses and maximum

deflection is located for each face of the enclosure. Hence, analytical conclusions were formed, which provided comparable results with the finite elements analysis software. An additional finite element analysis of the whole system without isolating the faces (all the plates joined together at the edges), provided interesting and comparable results. Meaning, for these exact conditions and loads, the uninsulated model presented similar behaviors and values compared to the fixed edges plate method for isolated plates, where further research on this topic behavior can be done.

Figure 15
The Integration of the Enclosure System with the Other Defined Subsystems

Both methods provided similar behaviors and served as the backbone of the optimization phase. Initially, the enclosure design without the reinforcement was having a maximum deflection of 0.497” and a maximum stress of 1.466E+05 Psi. However, with the same material (S.S.304), the reinforced enclosure with angular extrusion framing has a maximum deflection of 0.058”, which represents a decrease in deflection by 88.32%. As for stress, the reinforced system was experiencing a maximum stress value of 1.942E+04 Psi., which is below the yield strength (2.999E+04 Psi.) and provides a 1.54 minimum factor of safety (FOS). Additional to the compliance of the safety factor and the design of an enclosed system, the new enclosure provides viable manufacturing and cost efficiency. Thus, fabrication cost increased from $1,784 to $4,080 but was maintain below the $4,750 budget.

The development of the enclosure was constrained by the defined adjacent subsystems, timeframe, available manufacturing methods and a budget, which gave little room for creativity. However, these constraints, present interesting obstacles like building a rectangular vacuum vessel and developing an understanding on the mechanics of plates. The found relation between the mechanics of plates and a rectangular box, for the given assumptions and conditions, presents potential future research work. If the design project provided less constraints, then the enclosure would be designed vertically. In a vertical position, the dust that was removed by the jet air nozzles will be forced down by gravity to a concentrated small area. Therefore, this will help to maximize the efficiency of the dust collector machine and reduce suctions connections ports.

REFERENCES

[1] P. Anthony E. Armenàkas, *Advanced Mechanics of Materials and Applied Elasticity*, Boca Raton, Florida: Tylor & Francis Group, 2006.

[2] P. L. Gould and Y. Feng, *Introduction to Linear Elasticity*, 4th ed., Gewerbestrasse, Cham: Springer, 2018.

[3] A. P. Boresi and R. J. Schmidt, *Advanced Mechanics of Materials*, 6th ed., New Jersey: John Wiley & Sons, Inc., 2002.

[4] C. T. Wang, "Nonlinear Large Deflection Boundary-Value Problems of Rectangular," *Natl. Adv. Comm. Aeron.*, Tech. Note 1425, 1948.

[5] S. Levy, "Bending of Rectangular with Large Deflections," *Natl. Adv. Comm.*,Tech. Note 846, Washington, 1942.

[6] W. C. Young, R. G. Budynas and A. M. Sadegh, *Roark's Formulas for Sress and Strain*, 8th ed., New York, McGraw Hill., 2012.

[7] W. D. Callister and D. G. Rethwisch, *Material Science and Engineering: An Introduction*, 9th ed., Hoboken, NJ: Wiley, 2014.